

Dynamics of Dzyaloshinskii domain walls in ultrathin magnetic films

André Thiaville and Stanislas Rohart

Laboratoire de Physique des Solides, Univ. Paris-Sud, CNRS UMR 8502, 91405 Orsay Cedex, France

Émilie Jué

SPINTEC, UMR 8191, CEA/CNRS/UJF/Grenoble-INPG, INAC, 38054 Grenoble Cedex, France

Vincent Cros and Albert Fert

Unité Mixte de Physique CNRS-Thales and Univ. Paris-Sud, 91767 Palaiseau, France

We explore a new type of domain wall structure in ultrathin films with perpendicular anisotropy, that is influenced by the Dzyaloshinskii-Moriya interaction due to the adjacent layers. This study is performed by numerical and analytical micromagnetics. We show that these walls can behave like Néel walls with very high stability, moving in stationary conditions at large velocities under large fields. We discuss the relevance of such walls, that we propose to call Dzyaloshinskii domain walls, for current-driven domain wall motion under the spin Hall effect.

I. INTRODUCTION

Ultrathin magnetic films where the magnetic easy axis reorients to the film normal are one of the first systems in which the specificities of Nanomagnetism became visible. A surface contribution to the magnetic anisotropy of a sample was predicted early by L. Néel¹, and much later observed to dominate over the volume terms (anisotropy and magnetostatic) in films of thickness below 2 nm, typically, when such samples could be fabricated.

As the magnetic degrees of freedom along the film normal correspond to extremely high energy modes, such samples were assimilated to the practical realization of the model system in which the simplest magnetic domain wall (DW) exists, namely the Bloch wall^{2,3}. In this wall, the magnetization rotates as a spiral when one travels perpendicularly (direction x) across the DW, avoiding magnetostatic charges as $\text{div}\vec{m} = dm_x/dx = 0$, where \vec{m} is the unit vector defining the magnetization direction. The DW profile is thus governed by the exchange and anisotropy energies, the latter being in the ultrathin limit an effective anisotropy incorporating the perpendicular demagnetizing energy. As the typical DW widths are of a few nanometers, observations that the DW in such samples are of this type are extremely rare: spin-polarized scanning tunneling microscopy would require to control the orientation of the magnetic moment of the last atom, for example. The most convincing proof was recently obtained in nanostrips of (Co/Ni) multilayer by anisotropic magnetoresistance measurements, where for small nanostrip widths the DW structure was observed⁴ to transform into a Néel wall (NW), as expected from micromagnetics⁵. In the NW, the magnetization rotates in a cycloidal mode, i.e. with the DW normal x contained in the magnetization rotation plane. For perpendicular magnetization films that are not patterned into nanostrips, the BW does not have a magnetostatic energy but the NW does, so that indeed the BW is the lowest energy DW structure, justifying the common belief.

However, it was soon recognized that the energy den-

sity difference between NW and BW decreases as the film becomes thinner⁶, because the ‘demagnetizing factor’ of the NW reduces as the ratio $t \ln 2 / (\pi \Delta)$ of film thickness t to DW width $\pi \Delta$. A practical consequence of this is the low Walker field and maximum velocity of the BW in these films⁶. Indeed, the stability of a DW structure against precession around a field applied along the magnetization of the domains is what limits the stationary regime of DW motion, where the largest DW mobility (velocity to field ratio) and velocity are obtained. Another direct proof of this low stability of the BW in ultrathin films was recently obtained through the observation, by ballistic electron emission microscopy⁷, that in coupled films superimposed walls adopt an antiparallel NW structure. The stray field from the domains in one layer, despite its smallness because of the ultrathin film thickness, indeed overcomes the NW demagnetizing field in the other layer.

All these considerations rest on energy terms that are usually considered in micromagnetics. Recently, another term has been experimentally uncovered in the magnetism of mono- and bilayers, namely the Dzyaloshinskii-Moriya interaction (DMI)⁸⁻¹². This antisymmetric exchange interaction was introduced for low-symmetry crystals^{13,14}. It was shown to favor non-uniform magnetic structures¹⁵, prominently the nowadays so-called skyrmions. In the context of ultrathin films, A. Fert first mentioned that, the symmetry being reduced at the interface, such a term was also allowed¹⁶. This was confirmed by an extensive analytical study¹⁷ that considered the 2-site¹⁴ and 3-site¹⁸ mechanisms. Quantitative calculations of this interaction by ab initio techniques¹⁹ confirmed its importance for ultrathin films. Starting with the case of 2 monolayers Fe epitaxially grown on the W(110) surface of a single crystal, studied in depth by spin-polarized scanning tunneling microscopy²⁰, it was shown that the DMI changes the nature of the magnetic DW, forcing the existence of Néel walls¹⁰. The DW structure has also been investigated for general values of the parameters and orientation of the Dzyaloshinskii vector²¹, but in a

simplified model that does not solve the magnetostatic problem inherent to a Néel wall. Moreover, the practical consequences of the introduction of the DMI on the DW dynamics have not been investigated so far, with the exception of one work²² for a soft magnetic material with a DMI of bulk symmetry.

In this paper, we consider an ultrathin film with perpendicular easy axis, grown on a substrate with a capping from a different material so that the structural inversion symmetry is broken along the film normal (z axis), the typical sample being Pt/Co(0.6 nm)/AlOx²³. The film is patterned into a strip, elongated along the x axis, of a width below the micrometer but not as small as to induce by magnetostatics the transition to a Néel wall^{4,5}, providing a well-defined geometry to study the DW propagation. As the film is ultrathin, only the x - y degrees of freedom exist. The conventional micromagnetic energy density of the system is

$$\mathcal{E} = A \left[\left(\frac{\partial \vec{m}}{\partial x} \right)^2 + \left(\frac{\partial \vec{m}}{\partial y} \right)^2 \right] + K_u [m_x^2 + m_y^2] - \mu_0 M_s \vec{m} \cdot \vec{H}_a - \frac{1}{2} \mu_0 M_s \vec{m} \cdot \vec{H}_d. \quad (1)$$

In this expression, A is the (isotropic) exchange constant, K_u the uniaxial anisotropy constant with z the easy axis (sum of volume and surface anisotropies), M_s the spontaneous magnetization, \vec{H}_a is the applied field and \vec{H}_d the demagnetizing field computed from the magnetization distribution through the magnetostatics equations²⁴. In this geometry, we consider an interface DMI that reads in continuous form

$$\mathcal{E}_{\text{DMI}} = D \left[m_z \frac{\partial m_x}{\partial x} - m_x \frac{\partial m_z}{\partial x} \right] + \text{id. } (x \rightarrow y) \\ = D \left[m_z \text{div} \vec{m} - (\vec{m} \cdot \vec{\nabla}) m_z \right]. \quad (2)$$

This form corresponds to a sample isotropic in the plane, where the Dzyaloshinskii vector for any in-plane direction \vec{u} is $D \hat{z} \times \vec{u}$ with a uniform constant D , originating from the symmetry breaking at the z surface^{16,25}. This interface DMI differs from the bulk-like form where $\vec{D}[\vec{u}] // \vec{u}$. The expression (2) shows that indeed the DMI favors NWs of a given chirality, fixed by the sign of D .

The previous studies of the DW structure under interface DMI^{10,21} have only considered the statics ($\vec{H}_a = \vec{0}$) and neglected the complex effects of the demagnetizing field: either $\vec{H}_d = \vec{0}$ or a global demagnetizing effect was incorporated into an effective anisotropy. Here, we lift these two restrictions. Micromagnetic calculations are performed either in 2D (the full problem), or in a model reduced to 1D (along the x axis) but with a calculation of the demagnetizing field. We also show how part of the physics of this DW can be captured using the well-known collective coordinates approach (the so-called q - Φ model), with suitable modifications. Although most of the paper deals with field-driven motion of DW under DMI in ultrathin films, we finally discuss the relevance of the DMI to current-driven DW motion.

The micromagnetic parameters chosen for the simulations are those of the typical sample considered, namely $M_s = 1100$ kA/m, $A = 16$ pJ/m, $K_u = 1.27$ MJ/m³. This leads to a DW width parameter $\Delta = \sqrt{A/K_0} = 5.65$ nm where $K_0 = K_u - \mu_0 M_s^2/2$ is the effective anisotropy including the perpendicular demagnetizing field effect in the local approximation. For the magnetization dynamics, we use the gyromagnetic ratio of the free electron $\gamma_0 = 2.21 \times 10^5$ m/(A.s), and the damping factor $\alpha = 0.5$ that is the typical experimental value²⁶.

II. ONE-DIMENSIONAL MODEL

In a 1D model, the degrees of freedom transverse to the strip are quenched. As a result, the y derivatives in Eqs. (1), (2) disappear. Given the typical strip-width ($w = 500$ nm) compared to the sample thickness ($t = 0.6$ nm), we decide to neglect the y component of the demagnetizing field. In a first approximation, justified by the fact the nanostrip and DW widths are much larger than the sample thickness, we express the normal component of the demagnetizing field by the local approximation $H_{dz} = -M_s m_z$. The longitudinal component of the demagnetizing field is calculated by direct summation with interaction coefficients C_x analytically calculated (note also that the z component of the demagnetizing field can be calculated similarly, with coefficients C_z applied to m_z). As these interaction coefficients depend on the strip width w , this value has to be specified, even if its influence is very small. For the numerical results shown here, it was $w = 500$ nm. The numerical mesh size was 1 nm, and the length (in the x direction) of the calculation box was 300 nm. The box was shifted during the dynamic calculations in order to remain centered on the DW.

The main characteristics of the converged DW structures, as a function of the DMI parameter D , are shown in Fig. 1. The two DW moments (the integrated in-plane magnetization components, in nm) are plotted in Fig. 1a. They show that the transition from the BW at $D = 0$ to the NW at $D > D_c \approx 0.13$ mJ/m² is progressive. As we shall see below, this is an effect of the competition between the DMI and the magnetostatic energies. The variation of the DW energy, plotted in Fig. 1b, conforms with the analytic expectation $E = E_0 - \pi D^{10}$ at large D . Extrapolating the DW energy to zero, we see that this sample remains in the up-down state with domain walls up to $D_{\text{max}} \approx 3.7$ mJ/m², above which the nonuniform state develops.

Fig. 1c shows the variation of the DW width parameter Δ_T , using the Thiele definition of this parameter that directly applies to the DW dynamics²⁷. This parameter varies weakly, but the variation is a hint that an analysis with a Bloch wall profile is too simple. In order to see this, the profile of the x (Néel) magnetization component is plotted in Fig. 1d, and compared to the Bloch wall profile with this parameter Δ . The log scale

stresses that, although the Bloch wall profile is very accurate around the center of the wall, it does not describe the so-called tails that extend far from the DW. These tails, well-known in the in-plane case²⁴, are a direct consequence of the magnetostatic field inherent to the NW structure. Here, they are responsible for the increase of the wall width parameter Δ_T as the DW transforms to the NW, opposite to the naive expectations based only on the DW core energies.

We now study the dynamics of these DW structures under a field H_a applied along the easy (z) axis. As usual, a stationary motion with a high mobility is found at low field, followed by a lower velocity regime with a region of negative mobility just above the critical field called Walker field. Fig. 2a shows the $v(H_a)$ curves computed for various values of the DMI micromagnetic parameter D (in the precessional regime, as the changes are periodic, the average velocity is shown). The main effect of DMI is to extend the stationary regime, with no change of mobility. The curves are very similar to those of the standard $q - \Phi$ model for Bloch walls²⁸. In fact, comparing to the curves of that model with identical Walker field, Walker velocity and damping, some differences can be seen only in the intermediate field region with marked curvature. The value of the Walker field, plotted in Fig. 2b, shows a quasi linear increase with D .

The quantitative effect is very large: a value $D = 0.6 \text{ mJ/m}^2$ increases H_W by ten times compared to $D = 0$. The Walker velocity follows exactly the same trend, simply because the mobility in the stationary regime is constant ($1.96 \text{ m}/(\text{s.mT})$). Such a strong effect is physically intuitive: the DMI pins the DW magnetization to the Néel orientation, suppressing the precession of DW magnetization and thus extending the stationary regime to higher fields.

The robustness of the above results was tested by comparison to exact, but more demanding, 2D calculations (with suitably modified homemade²⁹ and OOMMF³⁰ codes), performed for different nanostrip widths $w \leq 500 \text{ nm}$ and $D < 0.5 \text{ mJ/m}^2$. As soon as w was larger than the BW-NW magnetostatic transition^{4,5}, the evolution of the results with w was minor. Neither a continuous rotation of the DW magnetization along the length of the wall, nor a tilt of the wall, were observed, so that the 1D model is justified, as it describes a stable structure. All quantities (DW width, Walker field, etc.) were found to be slightly modified, mainly because of the assumption of a local z demagnetizing field with $N_z = 1$, so that the effective anisotropy is larger and the DW width lower. The small variations, observed above the Walker field, are due to the transverse degrees of freedom (see Ref.³¹ for an example). They are more apparent as w or D increase. In order to give an idea of the magnitude of the 2D effects, one such calculation result is added in Fig. 2a.

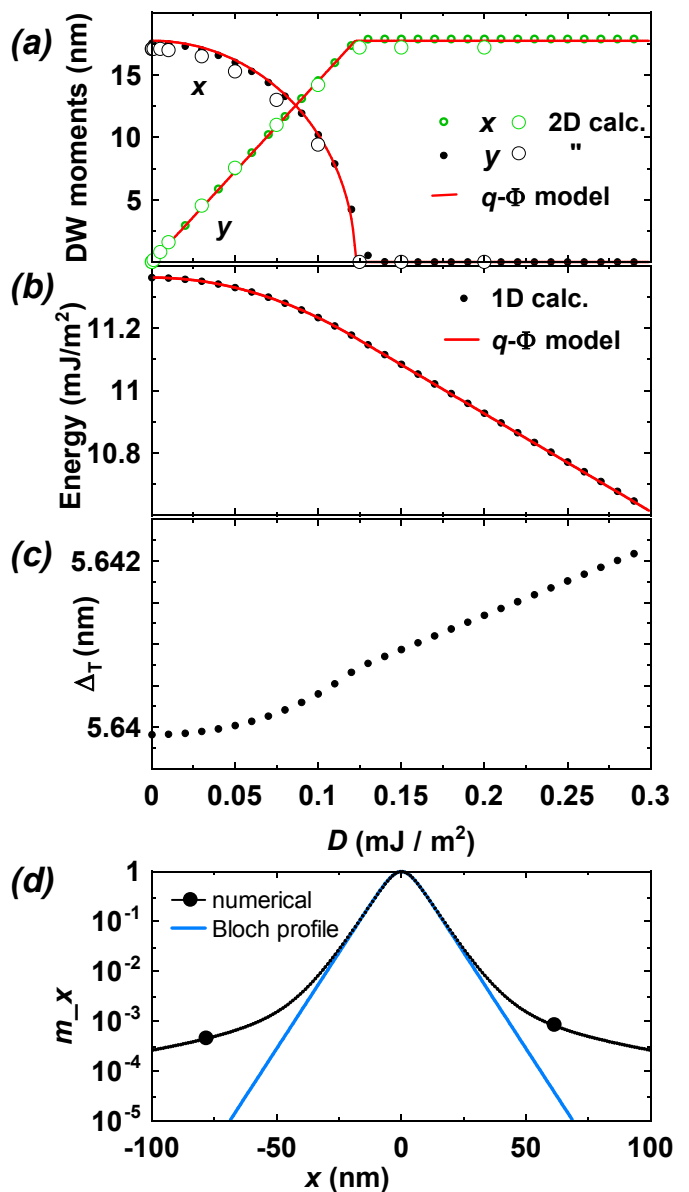


FIG. 1. Equilibrium DW structure according to the 1D model as a function of the magnitude of the DMI parameter D . (a) integrated DW magnetic moments for the x (Néel) and y (Bloch) components (big dots show the results of 2D calculation); (b) DW energy; (c) DW width according to the Thiele definition. The magnetization profile is plotted in (d) for the case $D = 0.2 \text{ mJ/m}^2$; it shows very little variation for larger values of D . Curves in (a,b) were obtained with the $q - \Phi$ model.

III. COLLECTIVE COORDINATES $q - \Phi$ MODEL

Despite the complexity of the NW profile (Fig. 1d), and of the local form of the DMI, a simplified model based on only two collective coordinates, namely the DW position q and the DW magnetic moment angle Φ , can be constructed, similarly to what has been done for the conventional DW²⁸. The starting point is to express the DW

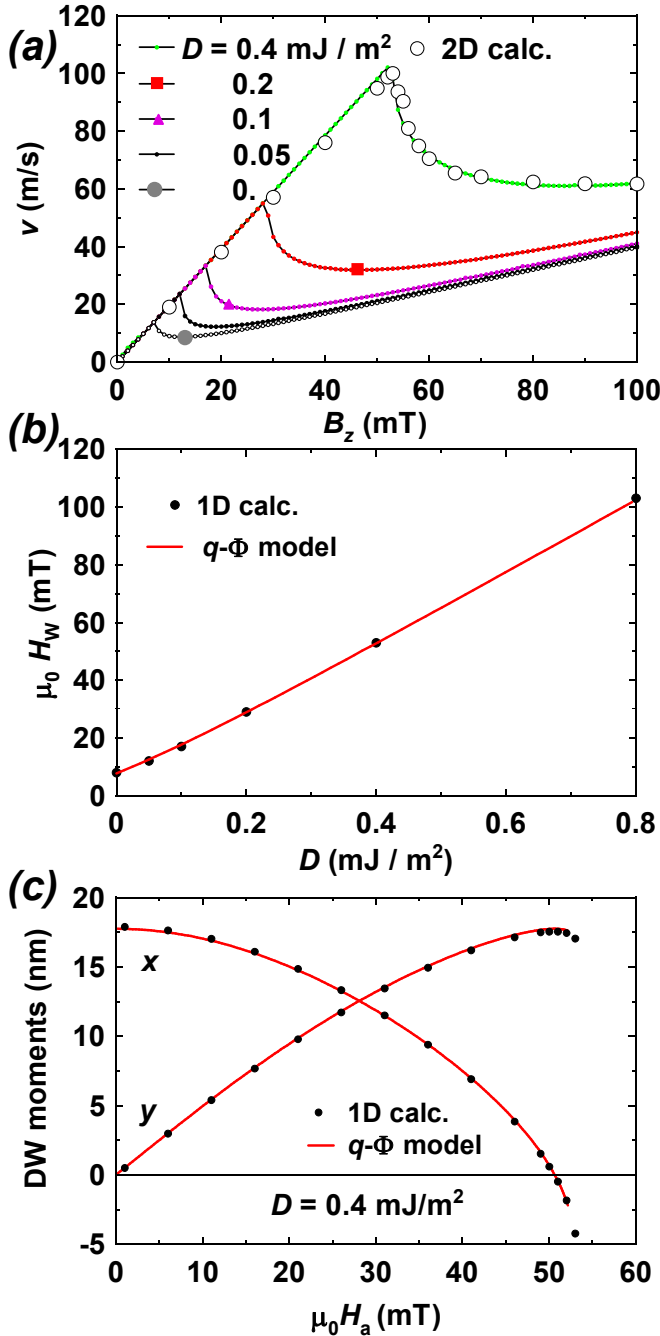


FIG. 2. Field-induced domain wall motion for different value of the DMI parameter D , as calculated by the continuous 1D model. (a) Velocity-field curves. The results of the 2D calculation for a width $w = 500$ nm and $D = 0.4$ mJ/m² are included for comparison (big dots). (b) Variation of the Walker field H_W with D . (c) Evolution of the two DW magnetic moments with field, in the stationary regime for $D = 0.4$ mJ/m². The curves in (b,c) show the results of the $q - \Phi$ model.

surface energy σ ³². As seen above, for the typical system that we consider the DW width is practically constant. We therefore assume that the wall width parameter is a constant $\Delta = \sqrt{A/K_0}$. We also make the assumption that the magnetization rotates in a vertical plane, rotated by an angle Φ around the z axis ($\Phi = 0$ for the NW). The 1D calculations show that this is not the case, neither far from the DW as m_x decays slowly whereas m_y does not, nor around the center of the wall when driven by a field. Nevertheless, this assumption allows a crucial simplification and the final results match quite well with 1D calculations, as shown below. In these conditions, the DW energy reads

$$\sigma = 2\Delta K \cos^2 \Phi - \pi D \cos \Phi + C^{\text{st}}, \quad (3)$$

where K is the magnetostatic ‘shape’ anisotropy that favors the Bloch wall, related to the ‘demagnetizing coefficient’ N_x of the wall by $K = N_x \mu_0 M_s^2 / 2$. The Slonczewski equations derived from Eq. (3) are then, with $H_K = 2K / (\mu_0 M_s)$ and $H_D = \pi D / (2\mu_0 M_s \Delta)$,

$$\dot{\Phi} + \alpha \dot{q} / \Delta = \gamma_0 H_a \quad (4)$$

$$\dot{q} / \Delta - \alpha \dot{\Phi} = \gamma_0 (-H_K \sin \Phi \cos \Phi + H_D \sin \Phi) \quad (5)$$

Minimizing σ with respect to Φ at $H_a = 0$ solves the statics. The stable solution is

$$\begin{aligned} \cos \Phi_0 &= \pi D / (4\Delta K) \text{ for } \pi |D| < 4\Delta K \\ &= \text{sign}(D) \text{ for } \pi |D| > 4\Delta K. \end{aligned} \quad (6)$$

Thus a critical value $D_c = 4\Delta K / \pi$ appears. When $|D| > D_c$ we have a NW, and below this limit the DW moment reorients smoothly to the Bloch orientation. Figs. 1a,b show the good overall agreement of this model with the numerical results of the 1D model (for all calculations with the $q - \Phi$ model, we used $\Delta = 5.64$ nm and $N_x = 0.0224$, derived from the 1D calculations).

The model is also analytically solvable in the stationary regime of the dynamics. Taking Φ as a parameter, one has indeed

$$H_a = \alpha \sin \Phi (H_D - H_K \cos \Phi). \quad (7)$$

Stability of Φ requires also that $H_K \cos 2\Phi - H_D \cos \Phi < 0$. The DW velocity v is then given by the stationary relation $v = (\gamma_0 \Delta / \alpha) H$, where. Fig. 2c shows how well this reproduces the numerical results of the 1D model for the case $D = 0.4$ mJ/m². The highest field applicable, the Walker field, is found to be given by $\cos \Phi_W = (\delta - \sqrt{\delta^2 + 8}) / 4$ where $\delta \equiv D / D_c = H_D / H_K$ (the expressions for the Walker field H_W and the Walker velocity v_W are cumbersome but straightforward to write; at large D one has simply $H_W \approx \alpha H_D$). The comparison with the Walker field data from the numerical solution of the 1D model is depicted in Fig. 2b, again with a very good agreement. In the precessional regime, the dynamic equation for Φ alone, derived from Eqs. (4),(5), should be integrated in order to get the oscillation period as

function of field. Comparison with the curve of the standard model ($D = 0$) shows some difference only in the regime where H_a is not so much above H_W , as may be anticipated.

IV. COMPARISON TO EXPERIMENTS

A first hint that the DW in ultrathin Pt/Co (0.6)/AlOx films is not a simple BW is provided by the DW dynamics under field only in this sample²³, compared to those of a series of Pt/Co(t)/Pt with $t = 0.5 - 0.8$ nm²⁶: the velocity in the flow regime is indeed at least 5 times larger in the former case (the comparison is not so direct as the Co/AlOx interface gives more interface anisotropy than the Co/Pt interface). The latter study concluded that the flow regime was precessional, with $\alpha \approx 0.3$, the stationary regime being hidden by the DW pinning. As a result, the high mobility observed for Pt/Co/AlOx can only be obtained in the stationary regime, but in that case the Walker field would be smaller than the fields applied (up to 120 mT). As shown by Fig. 2 and by the analytic model, this paradox can be lifted with $D \approx 1$ mJ/m² or larger. This value is reasonable: we estimate for Fe/W(110)¹⁰ 4 mJ/m², for Mn/W(001)⁹ 3 mJ/m², and for Fe/Ir(111)¹² 1.5 mJ/m², supposing a dilution of the DMI values found in mono- or bilayers over a 3 monolayers film.

One test of the NW structure due to DMI is to measure the DW dynamics under a z field, with an additional in-plane field along the x direction. Indeed, in simple terms, this field favours opposite chiralities for up-down and down-up walls, competing with the DMI. The results of the full 1D model for this case are shown in Fig. 3a, for an up-down wall with $D = +0.8$ mJ/m². The positive x fields add to the DMI for stabilizing the DW moment in the x orientation, and increase the Walker field (and Walker velocity). In the expression of the DW energy σ , the x field would enter like a DMI term, but the magnetization rotation that it induces in the domains should also be taken into account. This stresses the main interest of the DMI: it provides a large x field that exists only within the wall. The figure thus shows that $D = 0.8$ mJ/m² is equivalent to a stabilizing field $\mu_0 H_x \approx 128$ mT, which is exactly the value $D/(M_s \Delta)$ of the average over the DW of the equivalent B_x field deduced from Eq. (2). This is very different from the case of a transverse (y) field, where small changes of mobility and Walker field are observed, depending on the sign of the z field (not shown).

We proceed now to current-induced DW motion in ultrathin films with perpendicular anisotropy. Recent work^{33,34}, has revealed that the nature of the DWs in such samples is very important. Indeed, to explain the anomalously large DW velocity under current in Pt/Co/AlOx, a magnetic effect of the Rashba field at the interfaces has been proposed³⁵. On the other hand, a spin Hall effect (SHE) due to the current flowing in the Pt or

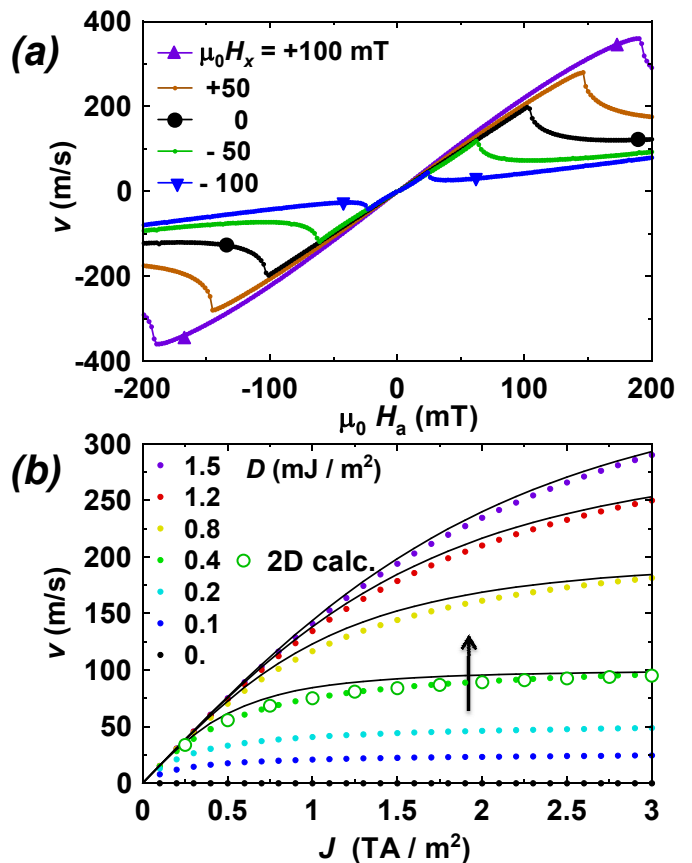


FIG. 3. Dynamics of a Dzyaloshinskii DW as calculated by the 1D model: (a) field-induced motion under an additional in-plane field along the nanostrip, for $D = 0.8$ mJ/m²; (b) current-induced motion due to the spin Hall effect in the underlayer, for a Hall angle $\theta_H = 0.1$ rad and several values of D , with results of 2D calculations superposed for one case (arrow depicts D increase, and curves show the large D solution of the extended $q - \Phi$ model).

Ta buffer layer has also been considered³⁶. The analysis of the action of these torques³³ shows that for perpendicular materials the SHE can efficiently move NWs at zero field and in opposite directions for opposite chiralities. This has been directly proven in the Pt/Co/Pt case³⁴, by preparing NW with moderate x fields and observing a current assisted depinning only for the NW. In that structure, the sign of the SHE was moreover controlled by the relative thicknesses of the two Pt layers, and a strong DMI is not expected as the effects of both interfaces compensate. We thus predict that, for asymmetric structures where the two interface DMI do not compensate, the DW may be a NW that efficiently moves under current by SHE, without the need of an applied field. Its direction of motion with respect to the current direction is given by the sign of the DMI parameter and the SHE film position (above or below the magnetic film). In addition, as the NWs induced by DMI have a fixed chirality, all walls will be pushed in the same direction under current by the SHE. This feature is highly desirable in

applications where one wants to obtain the motion of a train of DW in the same direction (race-track memory for example). It cannot be obtained with the opposite successive chiralities induced by an x field³⁴.

Calculations with the 1D model (Fig. 3b) indicate that DW velocity under SHE increases with D , becoming comparable to experiments²³ for $D > 1$ mJ/m² for a spin Hall angle of 0.1 rad. The $q - \Phi$ model can also be modified to include this term. Using the Thiele force equation approach, we find that the SHE can be input by an equivalent field $H_a = (\pi/2)\chi M_s \cos \Phi$, with $\chi = \hbar\theta_H J / (2e\mu_0 M_s^2 t)$ representing the SHE-induced STT³⁷, J being the current density. In the steady-state regime, and for $\delta \gg 1$ we obtain $v = v_D / \sqrt{1 + (J_D/J)^2}$, with $v_D = \gamma_0 \Delta H_D$ and $J_D = 2\alpha t e D / (\hbar\theta_H \Delta)$ (note that the v/J slope at $J = 0$ is independent of D). The agreement with the results of the full 1D model is good (Fig. 3b), despite the neglect of the magnetization rotation in the domains under the SHE.

V. CONCLUSION

We have studied by micromagnetics a new domain wall structure in ultrathin films with perpendicular

anisotropy, as a result of uncompensated Dzyaloshinskii-Moriya interactions from the adjacent layers, that we propose to call Dzyaloshinskii domain wall (DDW). Depending on the strength D of this interaction, domain wall magnetizations intermediate between the Bloch and Néel orientation are obtained, turning to Néel at large D . The motion of a DDW under field is strongly affected by D , with a nearly linear increase of Walker field and velocity with D , up to very large values before the domains become unstable. Specific features of the dynamics of the DDW under in-plane fields have also been described. DDWs offer an attractive scenario to contribute to the understanding of the wealth of experimental results on current-induced DW motion in ultrathin films with perpendicular anisotropy, and for applications.

ACKNOWLEDGMENTS

This work was supported by the Agence Nationale de la Recherche, project ANR 11 BS10 008 ESPERADO. Discussions with J. Vogel, G. Gaudin, S. Pizzini, I. M. Miron, O. Boulle and J. Miltat are gratefully acknowledged.

-
- ¹ L. Néel, J. Phys. Rad. **15**, 225 (1954).
² F. Bloch, Z. Phys. **74**, 295 (1932).
³ L. Landau and E. Lifshitz, Phys. Z. Sowjetunion **8**, 153 (1935).
⁴ T. Koyama, D. Chiba, K. Ueda, K. Kondou, H. Tanigawa, S. Fukami, T. Suzuki, N. Ohshima, N. Ishiwata, Y. Nakatani, K. Kobayashi, and T. Ono, Nature Mater. **10**, 194 (2011).
⁵ S.-W. Jung, W. Kim, T.-D. Lee, K.-J. Lee, and H.-W. Lee, Appl. Phys. Lett. **92**, 202508 (2008).
⁶ S. V. Tarasenko, A. Stankiewicz, V. V. Tarasenko, and J. Ferré, J. Magn. Magn. Mater. **189**, 19 (1998).
⁷ A. Bellec, S. Rohart, M. Labrune, J. Miltat, and A. Thiaville, Europhys. Lett. **91**, 017009 (2010).
⁸ M. Bode, M. Heide, K. von Bergmann, P. Ferriani, S. Heinze, G. Bihlmayer, A. Kubetzka, O. Pietzsch, S. Blügel, and R. Wiesendanger, Nature **447**, 190 (2007).
⁹ P. Ferriani, K. von Bergmann, E. Y. Vedmedenko, S. Heinze, M. Bode, M. Heide, G. Bihlmayer, S. Blügel, and R. Wiesendanger, Phys. Rev. Lett. **101**, 027201 (2008).
¹⁰ M. Heide, G. Bihlmayer, and S. Blügel, Phys. Rev. B **78**, 140403(R) (2008).
¹¹ S. Meckler, N. Mikuszeit, A. Pressler, E. Y. Vedmedenko, O. Pietzsch, and R. Wiesendanger, Phys. Rev. Lett. **103**, 157201 (2009).
¹² S. Heinze, K. von Bergmann, M. Menzel, J. Brede, A. Kubetzka, R. Wiesendanger, G. Bihlmayer, and S. Blügel, Nature Phys. **7**, 713 (2011).
¹³ I. E. Dzialoshinskii, Sov. Phys. JETP **5**, 1259 (1957).
¹⁴ T. Moriya, Phys. Rev. **120**, 91 (1960).
¹⁵ I. E. Dzyaloshinskii, Sov. Phys. JETP **20**, 665 (1965).
¹⁶ A. Fert, Materials Science Forum **59-60**, 439 (1990).
¹⁷ A. Crépieux and C. Lacroix, J. Magn. Magn. Mater. **182**, 341 (1998).
¹⁸ A. Fert and P. M. Levy, Phys. Rev. Lett. **44**, 1538 (1980).
¹⁹ M. Heide, G. Bihlmayer, P. Mavropoulos, A. Bringer, and S. Blügel, Newsletter of the Psi-K network **78** (2006).
²⁰ M. Bode, Rep. Prog. Phys. **66**, 523 (2003).
²¹ M. Heide, G. Bihlmayer, and S. Blügel, J. Nanoscience Nanotech. **11**, 3005 (2011).
²² O. A. Tretiakov and A. Abanov, Phys. Rev. Lett. **105**, 157201 (2010).
²³ I. M. Miron, T. Moore, H. Szambolics, L. D. Buda-Prejbeanu, S. Auffret, B. Rodmacq, S. Pizzini, J. Vogel, M. Bonfim, A. Schuhl, and G. Gaudin, Nature Mater. **10**, 419 (2011).
²⁴ A. Hubert and R. Schäfer, *Magnetic Domains* (Springer Verlag, Berlin, 1998).
²⁵ A. N. Bogdanov and U. K. RöSSLer, Phys. Rev. Lett. **87**, 037203 (2001).
²⁶ P. J. Metaxas, J.-P. Jamet, A. Mougin, M. Cormier, J. Ferré, V. Baltz, B. Rodmacq, B. Dieny, and R. L. Stamps, Phys. Rev. Lett. **99**, 217208 (2007).
²⁷ Y. Nakatani, A. Thiaville, and J. Miltat, J. Magn. Magn. Mater. **290-291**, 750 (2005).
²⁸ N. L. Schryer and L. R. Walker, J. Appl. Phys. **45**, 5406 (1974).
²⁹ J. Miltat and M. J. Donahue, "Handbook of magnetism and advanced magnetic materials," (Wiley, New York, 2007) pp. 742-764.

- ³⁰ OOMMF is a free software (in fact, an open framework for micromagnetics routines) developed by M.J. Donahue and D. Porter mainly, from NIST. It is available at <http://math.nist.gov/oommf>.
- ³¹ K. Yamada, J. P. Jamet, Y. Nakatani, A. Mougin, A. Thiaville, T. Ono, and J. Ferré, *Appl. Phys. Express* **4**, 113001 (2011).
- ³² J. C. Slonczewski, *Intern. J. Magnetism* **2**, 85 (1972).
- ³³ A. Khvalkovskiy, (2012), unpublished.
- ³⁴ P. P. J. Haazen, E. Murè, J. H. Franken, R. Lavrijsen, H. J. M. Swagten, and B. Koopmans, “Domain wall motion governed by the spin Hall effect,” (2012), arxiv:1209.2320.
- ³⁵ I. M. Miron, G. Gaudin, S. Auffret, B. Rodmacq, A. Schuhl, S. Pizzini, J. Vogel, and P. Gambardella, *Nature Mater.* **9**, 230 (2010).
- ³⁶ L. Liu, C. F. Pai, Y. Li, H. W. Tseng, D. C. Ralph, and R. Buhrman, *Science* **336**, 555 (2012).
- ³⁷ M. D. Stiles and J. Miltat, “Spin dynamics in confined magnetic structures iii,” (Springer, Berlin, 2006) pp. 225–308.